JOURNAL OF MAGNETIC RESONANCE **125,** 52–64 (1997)
ARTICLE NO. MN961085

The Methyl-Rotor Electron-Spin Dynamics in the Smoluchowski Drift-Diffusional Framework

ANDERS R. SØRNES*,† AND NIKOLAS P. BENETIS‡

*Department of Physics, University of Oslo, P.O. Box 1048 Blindern, N-0316 Oslo, Norway; and ‡Department of Physics and Measurement Technology, Linköping Institute of Technology, Linköping University, S-581 83 Linköping, Sweden

Received August 12, 1996; revised November 18, 1996

The EPR behavior of the internal motion of the methyl fragment in radicals is simulated using the Smoluchowski drift diffusion model. EPR stochastic Liouville lineshape calculations using this model are presented, allowing the exploration of the whole span of conditions between the discrete-site-exchange and the stepless-free-diffusion limits and offering a unification of these two approximate theories. An accurate value of the correlation time for the isotropic hyperfine interaction is calculated for the full ranges of the parameters describing the system and is compared to those given by the approximate models in the two limiting cases, allowing for a discussion of their quality. Long and short correlation time limit spectra are reported and interpreted using analytic models. For the isotropic hyperfine interaction studied here, no broadening effects are observed under Redfield (strong narrowing) conditions. This suggests absence of lifetime broadening effects in agreement with site-model results. The addition of a cos φ term in the hyperfine interaction is essential for pyramidal radical centres, as is demonstrated by simulation of experimental reports in the literature.

INTRODUCTION

The internal motion of the -CH_3 methyl fragment of a variety of radicals has over the years been subjected to numerous inquiries by EPR spectroscopists (*1–10*). At high temperatures, frequent random interaction with a reservoir at thermal equilibrium has been assumed, leading to stochastic models of the dynamics (*2, 4, 7, 9*). At low temperatures, a quantum mechanical rigid-rotor model (*5, 6, 8*) has been employed. EPR observable characteristics of this model distinguishing it from the stochastic models include mass dependence (*9*) and quantum effects such as tunneling. Models have been proposed that take both stochastic and deterministic effects into account (*8, 11*). The present work concerns the stochastic modeling of high-temperature experiments. In previous inquiries, two different stationary Markovian models have been considered, depending on the strength of the hindering potential compared to the temperature. A three-site exchange process has been applied to interpretation of experiments at temperatures much lower than the hindering potential barrier (*2, 4, 7, 9*). At temperatures exceeding the barrier, a free-diffusion Wiener–Einstein process has been used (*10*).

In early theoretical work by Freed and Fraenkel (*10*), the need for a model of diffusion in an external potential in this kind of problems was pointed out. The motivation for developing the program described here, which employs such advanced diffusional models, was the possibility of modeling experiments over a large temperature range involving a methyl rotor moving in a small potential.

A stochastic model frequently used in describing rotational relaxation in solution or liquid state EPR (*12–16*) is the Smoluchowski (*17*) process of diffusion in an external potential. This model allows the unification of the two previously used models, as both the free-diffusion and the site-exchange model are contained in it as special cases.

Consider in general a bounded hindering potential with several local minima. The Smoluchowski model expands into the Wiener–Einstein free-diffusion process when the potential barrier between the minima is greatly exceeded by the temperature. When the barrier exceeds the temperature, the model takes the form of an effective site-jumping model between potential minima, with the jump rate $1/\tau$ given by the Arrhenius relation

$$\frac{1}{\tau} \propto \exp\left[-\frac{(V_{\max} - V_{\min})}{kT} \right]. \qquad [1]$$

Here, $V_{\max}$ and $V_{\min}$ refer to the potential maxima and minima, respectively. This behavior of the model has been demonstrated mathematically for the case of bistable or monostable potentials and particular initial conditions (*18–22*). In the present work, it is observed even for periodic conditions and a C_{3v} potential, a result obtained by analytic and numerical methods.

† To whom correspondence should be addressed.

1090-7807/97 $25.00

In the present work, the Smoluchowski process is employed in modeling the internal motion of the methyl group in a radical of type $R-\dot{C}-CH_3$. The EPR lineshape calculation is achieved by incorporation of the model in the nonperturbative stochastic Liouville formalism introduced by Kubo (*23*) and refined by Freed (*24, 25*). The effective Lanczos algorithm (*26*) with reduced vector format of the complete Liouville matrix is employed (*27*).

GENERAL THEORY

The theoretical EPR lineshapes presented in this work are calculated within the stochastic Liouville equation (SLE) framework. The expression for the continuous wave (CW) EPR lineshape is worked into the equivalent but more convenient form of the free-induction-decay (FID) (*27*) lineshape, where the initial density operator is obtained by a rotation of the equilibrium density $\pi/2$ about the y axis, thus rendering it approximately proportional to S_x at high temperatures. The lineshape expression is (*27*)

$$I(\omega) = \mathrm{Re}\langle S_+ \rho(\omega)\rangle, \qquad [2]$$

where $\rho(\omega)$ is the Fourier Laplace (FL) transform of the density operator. It is obtained from the SLE (*23–25*)

$$\frac{\partial \rho(t)}{\partial t} = (-i\mathcal{H}^{\times} + \Gamma)\rho(t). \qquad [3]$$

The notation $\mathcal{H}^{\times} = [\mathcal{H}, \cdots]$ is used, where $\mathcal{H}$ is the Hamiltonian. Γ is the Fokker–Planck (FP) operator for the stochastic process employed and will be defined below. FL transformation of [3] yields

$$(i\mathcal{H}^{\times} - \Gamma - i\omega)\rho(\omega) = \rho(0). \qquad [4]$$

Denoting by $|A)$, $|B)$ the linear operators A, B in the Liouville space with the inner product

$$(A|B) = \mathrm{Tr}(A^{+}B), \qquad [5]$$

the lineshape expression becomes

$$I(\omega) = \mathrm{Re}\left(S_- \left| \frac{1}{i\mathcal{H}^{\times} - \Gamma - i\omega} \right| \rho_0 \right). \qquad [6]$$

Here, $\rho_0 = \rho(0)$ is the initial density operator. Let $P(\varphi_0|\varphi, t)$ be the conditional probability distribution function. Then, the Fokker–Planck equation for the process is

$$\frac{\partial P(\varphi_0|\varphi, t)}{\partial t} = \Gamma P(\varphi_0|\varphi, t). \qquad [7]$$

The initial density operator is assumed separable in motional and spin degrees of freedom. Assuming the stochastic variable is initially distributed at equilibrium, the overall FID initial density operator is $\rho_0 \sim P_0 S_x$, where P_0 is the stationary solution to [7].

The Fokker–Planck equation employed is the Smoluchowski (*17*) equation

$$\Gamma = \frac{1}{\xi}\left(\frac{\partial^2 V}{\partial \varphi^2} + \frac{\partial V}{\partial \varphi}\frac{\partial}{\partial \varphi} + kT\frac{\partial^2}{\partial \varphi^2} \right). \qquad [8]$$

Here, $V(\varphi)$ is the potential energy of the rotor and ξ is the friction coefficient; $\xi = \tau/\omega$ if τ is the dissipative torque and ω is the angular velocity of the rotor. An important feature of the process, distinguishing it from the quantum mechanical model of motion, is the independence of the moment of inertia of the rotor. However, it is a projected process, and the conditions for the validity of the approximation it constitutes are inertial dependent (*28, 29*).

The FP operator Γ is not in general hermitian, but can always be cast into hermitian form by virtue of the transformation (*15*)

$$\tilde{\Gamma} = P_0^{-1/2}\Gamma P_0^{1/2}, \quad \tilde{\rho}(\omega) = P_0^{-1/2}\rho(\omega),$$
$$P_0(\varphi) = \frac{1}{Z}e^{-V(\varphi)/kT}, \quad Z = \int e^{-V(\varphi)/kT}d\varphi. \qquad [9]$$

The transformed FP operator is

$$\tilde{\Gamma} = \frac{1}{\xi}\left\{ \frac{1}{2}\left[\frac{\partial^2 V}{\partial \varphi^2} - \frac{1}{2kT}\left(\frac{\partial V}{\partial \varphi} \right)^2 \right] + kT\frac{\partial^2}{\partial \varphi^2} \right\}. \qquad [10]$$

Submitting the FL transformed SLE to this transformation, and inverting and subsequently resubstituting $\rho(\omega)$ yields

$$\rho(\omega) = P_0^{1/2}\frac{1}{i\mathcal{H}^{\times} - \tilde{\Gamma} - i\omega}P_0^{1/2}\rho(0). \qquad [11]$$

The lineshape expression now becomes (*15*)

$$I(\omega) = \mathrm{Re}(S_- P_0^{1/2}\left| \frac{1}{i\mathcal{H}^{\times} - \tilde{\Gamma} - i\omega} \right| P_0^{1/2}S_x). \qquad [12]$$

The Hamiltonian considered here is the spin Hamiltonian of a p electron interacting with the β-position methyl group protons. The hyperfine interaction is approximated by its isotropic component $2a\cos^2\varphi$. The Hamiltonian is then given by

$$H = \omega_{0S} S_z - \sum_{n=-1}^{1} \omega_{0I} I_{n_z} + \sum_{n=-1}^{1} \frac{a}{2} (\epsilon_n^* e^{i2\varphi} + \epsilon_n e^{-i2\varphi} + 2)\mathbf{S}\cdot\mathbf{I}_n. \quad [13]$$

Here,

$$\epsilon_n = e^{i(2\pi/3)n}. \quad [14]$$

The orientational $\cos^2\varphi$ hyperfine-interaction term has been expanded in irreducible tensors of the symmetry group of the operator Γ, C_{3v} (cf. Appendix A).

In radicals deviating from sp^2 hybridization of the radical center, it is found that the term $a_1 \cos\varphi$ or

$$\sum_{n=-1}^{1} \frac{a_1}{2} (\epsilon_n e^{i\varphi} + \epsilon_n^* e^{-i\varphi})\mathbf{S}\cdot\mathbf{I}_n \quad [15]$$

must be added to the hyperfine coupling (*30*). It will be shown that this term is necessary in some cases to produce correct spectra for ''stopped'' rotors.

It is evident from examination of the Hamiltonian that the SLE does not couple S_- and S_+. Thus, the lineshape expression can be cast into the form of a diagonal element of the inverted FL-transformed stochastic Liouville matrix (SL) suitable for direct use with the Lanczos algorithm (*15*):

$$I(\omega) = \mathrm{Re}\left(S_- P_0^{1/2} \left| \frac{1}{iH^{\times} - \tilde{\Gamma} - i\omega} \right| P_0^{1/2} S_- \right). \quad [16]$$

A standard choice (*11, 31*) for the hindering C_3 potential is

$$V(\varphi) = \frac{1}{2} V_3 \{1 - \cos[3(\varphi - \delta)]\}. \quad [17]$$

Although no additional difficulty is introduced into calculations by incorporating δ in treating this type of potential, an equivalent, but more convenient, method is used in the present work. A new angle $\varphi' \to \varphi = \varphi' - \delta$ is substituted, introducing the offset angle $+\delta$ in the hyperfine term of the Hamiltonian, but leaving δ out of the FP operator, which then becomes

$$\tilde{\Gamma} = \frac{9V_3}{4\xi} \cos 3\varphi + \frac{9V_3^2}{32\xi kT} \cos 6\varphi - \frac{9V_3^2}{32\xi kT} + \frac{kT}{\xi} \frac{\partial^2}{\partial\varphi^2}. \quad [18]$$

The numerical methods employed for inversion are greatly simplified if the SL operator is complex symmetric. This can be achieved if an orthonormal basis of real functions is used. The real Fourier series basis of sines, cosines, and a constant is adequate for this purpose:

$$\left\{ \frac{1}{\sqrt{\pi}} \sin(m\varphi) \mid m \in \mathbb{N} \right\}, \left\{ \frac{1}{\sqrt{\pi}} \cos(m\varphi) \mid m \in \mathbb{N} \right\}, \frac{1}{\sqrt{2\pi}}. \quad [19]$$

In the following, the sines are labeled by negative and the cosines by positive values of m (cf. Appendix B).

In order to conveniently use the lineshape expression after algebraic inversion of the Liouvillean, the distribution $P_0^{1/2}$ should be expanded in the real Fourier basis. As the $C_{3v}A_1$ symmetry indicates, the expansion is

$$e^{-[V_3(1-\cos 3\varphi)]/4kT} = \frac{1}{\sqrt{2\pi}} c_0 + \sum_{k=0}^{\infty} c_{3k} \frac{1}{\sqrt{\pi}} \cos(3k\varphi). \quad [20]$$

The expansion coefficients $\{c_{3k}\}$ are

$$c_{3k} = 2\sqrt{\frac{\pi}{1 + \delta_{k,0}}}\, e^{-V_3/4kT} \sum_{\mu=0}^{\infty} \frac{(V_3/8kT)^{2\mu+k}}{\mu!(\mu + k)!}, \quad [21]$$

which can be related to the integer order associated Bessel (*32*) functions $I_m(V_3/4kT)$:

$$c_{3m} = 2\sqrt{\pi} e^{-V_3/4kT} I_m\left(\frac{V_3}{4kT}\right),$$

$$c_0 = \sqrt{2\pi} e^{-V_3/4kT} I_0\left(\frac{V_3}{4kT}\right). \quad [22]$$

THE TRUNCATION PROBLEM

The motional basis is, in principle, of infinite dimension. However, for most problems the lineshape expression calculated from an increasing finite basis converges at some point, leaving the lineshape insignificantly dependent on the remaining basis functions. The SL matrix may thus, in practice, be truncated at some finite dimension.

The problem of finding the appropriate truncation level may be solved by comparing spectra calculated using an increasing number of basis functions and checking for convergence using a root-mean-square criterion. However, as this is computationally time consuming, an *a priori* method of finding the appropriate truncation dimension is sought. It is shown below that, using real Fourier basis functions with

increasing label number $|m|$ (cf. Appendix B), convergence at some point is obtained.

Three effects must be taken into account: (i) the expansion of the square root of the equilibrium density function $P_0^{1/2}$; (ii) the off-diagonal elements of the SL matrix introduced by the hyperfine interaction; (iii) the off-diagonal elements of the SL matrix introduced by the potential. The last effect is considered first.

By inspection of the FP operator, it is observed that if the basis function label number m is numerically large, then the real Fourier basis functions become eigenvectors of the FP operator, with eigenvalue:

$$\lambda_m^{(0)} = -\frac{kT}{\xi} m^2 - \frac{9V_3^2}{32\xi kT}. \qquad [23]$$

When $|m|$ is slightly smaller, so that the off-diagonal elements are nonvanishing, yet much smaller than the diagonal elements, second-order perturbation theory may be used, giving the following correction to the eigenvalue:

$$\lambda_m^{(2)} = \sum_{k(\neq m)} \frac{|\langle m|\tilde{\Gamma}|k\rangle|^2}{\lambda_m^{(0)} - \lambda_k^{(0)}} = -\frac{81V_3^2}{32\xi kT} \times \left(\frac{1}{4m^2 - 9} + \frac{V_3^2}{256(kT)^2}\frac{1}{m^2 - 9}\right). \qquad [24]$$

The assumption is made that if $\lambda_m^{(2)}/\lambda_m^{(0)} \ll 1$, then the basis function of label m is effectively an eigenfunction of the stochastic operator and does not mix with any other basis vector.

The lineshape expression depends on the elements of the inverted SL matrix corresponding to nonvanishing components of $P_0^{1/2}$. If the expansion of $P_0^{1/2}$ converges at some dimension k, then if $|m| > k$, the basis vector m affects the lineshape only through its coupling with k. If $\lambda_m^{(2)}/\lambda_m^{(0)} \ll 1$ is true for m, then the coupling is weak and the lineshape is not affected by the removal of m from the basis.

Calculating with respect to orders of magnitude and assuming $V_3 \gg kT$, the criterion becomes

$$|m| \gg \frac{V_3}{kT}. \qquad [25]$$

These suggestions are supported by numerical investigations. It is observed that the ground state eigenvalue found by diagonalizing the A_1 block approaches zero only after a sufficient number of basis functions have been employed. A numerical diagonalization of the A_1 block for an increasing number of basis functions was carried out, and the numerically lowest eigenvalue was checked for convergence. The results support the above assumption.

The effect of the hyperfine coupling term of the Hamiltonian must also be considered, as it introduces off-diagonal elements in the SL matrix on the same order of magnitude as the hyperfine coupling a. Employing the above methods, it is observed that the truncation level should in this case always be chosen so that

$$|m| \gg \sqrt{\frac{a}{D}}. \qquad [26]$$

Here, $D = kT/\xi$ is the diffusion constant. To summarize, the three criteria that all must be fulfilled for the mth basis function to be removed from the calculation of the lineshape are that, first, $|m|$ should exceed the convergence level of the equilibrium distribution. Second, taking into account the stochastic part of the SL, Γ, $|m|$ should exceed V_3/kT. Finally, taking into account the total SL, $|m|$ should also exceed $(a/D)^{1/2}$.

The Site-Exchange Model Approximation

By introducing the two independent variables $\lambda = V_3/kT$ and $D = kT/\xi$, the transformed Smoluchowski operator [18] becomes

$$\tilde{\Gamma} = -D\left(-\frac{9}{4}\lambda\cos 3\varphi - \frac{9}{32}\lambda^2\cos 6\varphi + \frac{9}{32}\lambda^2 - \frac{\partial^2}{\partial\varphi^2}\right). \qquad [27]$$

There are two independent parameters in the Smoluchowski equation, D and λ. It will be shown that the latter can be pictured as the ''switch'' between two approximate stochastic models. If $\lambda \gg 1$, the motion is characterized by random jumps between potential minima, as in a site-exchange process. If $\lambda \ll 1$, the motion approaches that of a free-diffusion process.

The parameter D, which only affects the eigenvalues of the stochastic operator linearly and does not affect the eigenvectors, simply scales the time variable of these processes. This can be observed by the rewriting [7] as

$$\frac{\partial P}{\partial(Dt)} = (D^{-1}\Gamma)P. \qquad [28]$$

Here, $(D^{-1}\Gamma)$ is independent of D and t.

The development of the Arrhenius expression for site exchange from the Smoluchowski equation with potential wells has been a problem of long-standing interest (*18–22*).

Kramers (*18*) employed a bistable potential with absorbing walls. Blomberg (*20*) considered a double-harmonic-oscillator potential. Weaver (*21*) used integration techniques with a monostable potential with one absorbant and one reflective boundary condition. Dattagupta (*22*) employed the variational principle with a bistable potential.

In need of a theory taking into consideration periodic boundary conditions of more than two potential wells, a somewhat different approach is employed here. A general expression for the conditional probability density (*15*) is

$$P(\varphi_0|\varphi t) = \sqrt{\frac{P_0(\varphi)}{P_0(\varphi_0)}} \sum_m G_m^*(\varphi_0) G_m(\varphi) e^{\gamma_m t}, \quad [29]$$

where $G_m(\varphi)$ and γ_m are the mth eigenvector and eigenvalue of $\tilde{\Gamma}$, respectively.

When $\lambda \gg 1$, P_0 can be approximated by a Gaussian representation of a delta function about $\varphi = 0$ and $\pm 2\pi/3$. The eigenvectors of Γ are negligible except in the proximity of these locations. This motivates an approach widely used (*5, 11*) in the study of the tunneling rate in the quantum mechanical rotor model, namely, the second-order expansion of the potential about each of these locations. Fjeldsø (*34*) employed the method in a problem of a supersymmetric quantum pendulum of slightly different symmetry, but which is otherwise mathematically equivalent to the Smoluchowski diffusion problem considered here.

It will be shown below that this treatment is not directly applicable for quantitatively determining jump rates, due to the overestimation of the potential barrier height caused by the second-order approximation of the potential around each potential well. This is also expected to be the case in the quantum mechanical model: The harmonic oscillator functions derived from a second-order potential expansion will not produce correct tunneling frequencies.

In the case studied here, adjustments will be made, making it possible to extract the exponential behavior of the jump rate predicted by the Arrhenius relation (*18–22*) at the cost of the accuracy of the preexponential factor. By expanding $\cos 3\phi$ and $\cos 6\phi$ about locations $\phi = 0, \pm 2\pi/3$ and retaining terms up to second order, the eigenvalue equation of $\hat{\Gamma} = -D^{-1}\tilde{\Gamma}$ is converted into the form of a quantum mechanical harmonic oscillator Hamiltonian (The constant $-9\lambda/4$, for which the only effect is an addition to the eigenvalues, has been removed from $\hat{\Gamma}$ for clarity.)

$$\hat{\Gamma} = -\frac{\partial^2}{\partial\varphi^2} + \beta^2\left(\varphi - \frac{2\pi n}{3}\right)^2, \quad n = 0, \pm 1. \quad [30]$$

Here, $\beta = \frac{9}{4}\sqrt{\lambda(\lambda+2)}$.

As will be explained below, only the smallest eigenvalue needs to be considered here, although the extension of the procedure is trivial (*34*). The three degenerate solutions are thus ground state harmonic oscillators in each of the three potential wells. Each solution can be made periodic by shifting the argument by 2π any number of times and summing the resulting functions. The result is

$$f_n(\varphi) \propto \sum_{m=-\infty}^{\infty} e^{-(1/2)\beta(\varphi - 2\pi n/3 + 2\pi m)^2}, \quad n = 0, \pm 1. \quad [31]$$

Note that the index n refers to the potential well in which the wavefunction is centered. For $\beta \gg 1$, [31] can be approximated by the mathematically more convenient

$$f_n(\varphi) \propto e^{\beta\cos(\varphi - 2\pi n/3)}, \quad n = 0, \pm 1. \quad [32]$$

This can be observed by second-order Taylor expansion of the cosine function and has been shown by Villain to be valid by Fourier coefficient comparison (*33*).

It is observed that, in the approximation of harmonic oscillator potentials, the ground state $\{f_n\}$ is triply degenerate. Appropriate zero-order perturbation theory eigenfunctions are found by diagonalizing $\hat{\Gamma}$ in this basis. Labeling diagonal terms as $\alpha = \langle f_n|\hat{\Gamma}|f_n\rangle$ and off-diagonal terms as $V = \langle f_n|\hat{\Gamma}|f_m\rangle$, $m \neq n$, the result is

$$G_{\mathrm{A}} = \frac{1}{\sqrt{3}}(f_{-1} + f_0 + f_{+1}), \quad \hat{\gamma}_{\mathrm{A}} = \alpha + 2V,$$

$$G_{\mathrm{E}_a} = \frac{1}{\sqrt{3}}(f_{-1} + \epsilon^* f_0 + \epsilon f_{+1}), \quad \hat{\gamma}_{\mathrm{E}_a} = \alpha - V,$$

$$G_{\mathrm{E}_b} = \frac{1}{\sqrt{3}}(f_{-1} + \epsilon f_0 + \epsilon^* f_{+1}), \quad \hat{\gamma}_{\mathrm{E}_b} = \alpha - V. \quad [33]$$

Here, $\epsilon = \exp(i2\pi/3)$. The ground state eigenvalue of Γ, γ_{A}, is known from theory to be zero. Requiring this, the result is $\gamma_{\mathrm{E}_a,\mathrm{E}_b} = -D\hat{\gamma}_{\mathrm{E}_a,\mathrm{E}_b} = 3VD$.

Neglecting all larger eigenvalues from excited harmonic oscillator states, their influence on the conditional probability being transient over the time scale of the observation, [29] and [33] give

$$P(k|mt) = G_{\mathrm{A}}(k)G_{\mathrm{A}}(m) + \mathrm{e}^{3VDt}(G_{\mathrm{E}_a}(k)G_{\mathrm{E}_a}(m) + G_{\mathrm{E}_b}(k)G_{\mathrm{E}_b}(m)], \quad [34]$$

where k (and m) specify the potential well $\phi = 2\pi k/3$. Assuming further that the $f_n(\phi = 2\pi m/3) \propto \delta_{mn}$ and normalizing P, combining [33] and [34] gives

$$P(k|mt) = \frac{1}{3}(1 - e^{-3|V|Dt}) + e^{-3|V|Dt}\delta_{km}, \quad [35]$$

which is the conditional probability for a three-site exchange process of jump rate $1/\tau = |V|D$ (*39*). The overlap integral V can be calculated from the normalized basis functions [32] by Fourier expansion. The result is

$$\langle f_m|\hat{\Gamma}|f_n\rangle = -\frac{9\lambda^2}{32}I_6(\beta) + \frac{9\lambda}{4}I_3(\beta) - \frac{\beta^2}{4}I_2(\beta) + \frac{\beta}{2}I_1(\beta) + \left(\frac{9\lambda^2}{32} - \frac{\beta^2}{2}\right)I_0(\beta) = \frac{}{I_0(2\beta)}, \quad m \neq n. \quad [36]$$

The asymptotic approximation

$$I_m(\beta) \xrightarrow[\beta \gg m]{} \frac{1}{\sqrt{2\pi\beta}}e^{\beta}$$

of the modified Bessel functions (*32*) gives

$$\langle f_m|\hat{\Gamma}|f_n\rangle = \left(-\frac{3}{4}\beta^2 + \frac{1}{2}\beta + \frac{9}{4}\lambda\right)\sqrt{2}e^{-\beta}, \quad m \neq n. \quad [37]$$

This equation has the negative exponential form parallel to the Arrhenius relation (*18–22*).

Using the value $\beta \approx 9\lambda/4$ obtained from the original expansion of the harmonic terms in $\hat{\Gamma}$, leading to [30], results in a gross overestimate of the magnitude expected for the exponent λ. As has already been pointed out, the reason for the failure is that the harmonic oscillator approximation gives an overestimate of the actual barrier height.

Adjusting the harmonic oscillator frequency so that the approximated potential consists of neighboring parabolas still centered at the potential minima, but now intersecting each other at the exact height of the actual cosine barrier, provides a periodic C_{3V} bounded model potential of correct barrier height, although the geometry near the potential minima is poorly approximated.

Two neighboring parabolas separated by $2\pi/3$, e.g., $y = c\varphi^2$ and $y = c(\varphi - 2\pi/3)^2$, intersect each other at the height $y = c\pi^2/9$. If this approximate barrier height is set equal to the actual cosine potential barrier height, V_3, then $c = 9V_3/\pi^2$. Retaining only terms of second order in λ, and inserting the parabolic potential approximation into [27], the form of Eq. [30] is again achieved, but with an adjusted frequency $\beta = 9\lambda/\pi^2$. This value is rather close to the expected λ. Assuming $\beta \approx \lambda$ gives the jump rate

$$\frac{1}{\tau} \approx -VD \approx \left(\frac{3}{4}\lambda^2 - \frac{11}{4}\lambda\right)\sqrt{2}De^{-\lambda}. \quad [38]$$

The second-order term dominating the preexponential factor was not expected (*18–22*). Therefore, numerical investigations were made.

A logarithmic plot of the lowest nonzero eigenvalue of $\hat{\Gamma} = -\tilde{\Gamma}/D$, i.e., $3|V|$, as a function of λ obtained by numerical diagonalization is shown in Fig. 1. The result was fitted

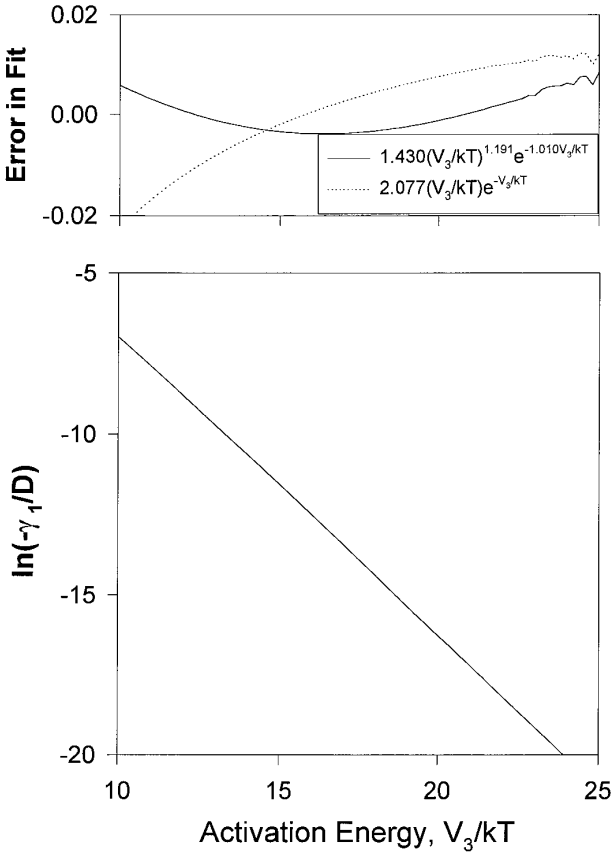

FIG. 1. The lowest nonzero eigenvalue of the Smoluchowski Fokker–Planck operator for one-dimensional Brownian motion in a C_{3v} harmonic potential. The natural logarithm of the negated eigenvalue is plotted against the activation energy, V_3, scaled in units of absolute temperature, kT. The eigenvalue is scaled in units of D. The plot reveals the negative exponential behavior predicted by the Arrhenius relation (*18–22*). Fitting the data to the expression $a(V_3/kT)^b\exp(-cV_3/kT)$ resulted in the values $a = 1.430$, $b = 1.191$, and $c = 1.010$, the error being within the resolution of the figure. Forcing the data into the more commonly assumed (*9, 18–22*) expression $a(V_3/kT)\exp(-V_3/kT)$ resulted in $a = 2.077$, the error still being within the resolution of the figure. The differences between each of the two fitting functions and the data are displayed in the top figure.

to an expression of the form $(a\lambda + b\lambda^2)\exp(-c\lambda)$, giving $a = 1.77$, $b = 0.0780$, and $c = 1.02$, which is in acceptable correspondence with the expected negative exponential behavior. However, the preexponential factor is not well represented by the above calculations, the most serious inconsistency being the second-order λ dependence in [38]. This is to be expected due to the severe discrepancy between the approximate and the exact potential in the regions close to the potential minima, where the exact form of the potential is crucial to the eigenproblem.

A fit to the more generally assumed expression (*18–22*) $a\lambda e^{-\lambda}$ gave $a = 2.08$. The error in this fit is small enough to be unresolved at the resolution of Fig. 1.

To summarize, it is observed that the exponential dependence [1] of the jump rate on the potential height is also valid in a C_{3V} periodic potential of three intersecting parabolas, where the barrier height is considered to be the height of the intersection between neighboring parabolas. In a cosine potential, [1] is observed to still hold, while the preexponential factor is changed from a second-order potential dependency to a first-order potential dependency. Furthermore, it is observed that employing a second-order expansion of the potential about each potential minimum does not produce numerically correct jump rates (or tunneling rates in the similar quantum-mechanical model).

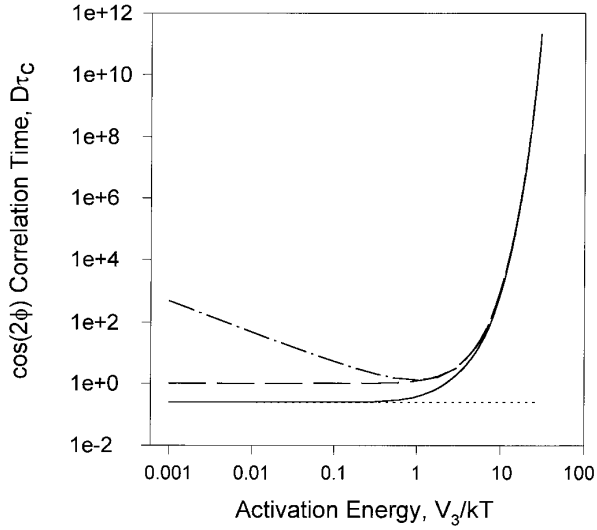

FIG. 2. The cos 2φ correlation time in the one dimensional Smoluchowski model of Brownian motion in a C_{3v} harmonic potential (—), scaled with the inverse diffusion constant D^{-1}, plotted against the activation energy scaled with absolute temperature, V_3/kT. It is compared to the correlation time predicted by the free-diffusion model (· · ·), $\tau_c = 1/4D$, and that predicted by the jump model, $\tau_c = 1/(-\gamma_1)$, either assuming the first nonvanishing eigenvalue to be of the Arrhenius (-·-·-·-) form (*9, 18–22*), $-\gamma_1 = 2.077D(V_3/kT)\exp(-V_3/kT)$, the exact numerical constants taken from Fig. 1, or calculating the exact value of γ_1 numerically (---).

Correlation Time

In the discussion below, the correlation time of the cos 2φ part (*10*) of the hyperfine coupling is needed, as this is the time scale of the motional averaging of the coupling. The correlation time is in general the motional-dynamics characterization parameter sought in relaxation and lineshape studies. The correlation time is calculated here for a general choice of parameters in the Smoluchowski process employed in this work using the following numerical procedure.

Consider the correlation time expression for an arbitrary orientation-dependent function $g[\varphi(t)]$:

$$\tau_c = \frac{1}{\langle g^2\rangle}\int_0^\infty \langle g(0)g(t)\rangle dt = \frac{\Sigma_m\, g_m(1/-\gamma_m)}{\Sigma_m\, g_m}. \quad [39]$$

Here, γ_m are the eigenvalues of the FP operator, $\Gamma P_m = \gamma_m P_m$. The numbers g_m are defined according to

$$g_m = \int d\varphi_0 P_0^{-1/2}(\varphi_0) G_m^*(\varphi_0) P(\varphi_0) g(\varphi_0) \times \int d\varphi P_0^{1/2}(\varphi) G_m(\varphi) g(\varphi), \quad [40]$$

and are independent of D. It is assumed that $g(\varphi)$ is chosen so that $g_0 = 0$. Equation [40] follows from the expansion of the delta function and the conditional probability into the eigenfunctions of the FP operator Γ. Since $-\gamma_m \propto D$, then $\tau_c \propto D^{-1}$. Choosing the probability distribution at time $t = 0$ to be the equilibrium distribution $P_0(\varphi)$ and assuming real eigenvectors gives

$$g_m = \left[\int d\varphi P_0^{1/2}(\varphi) G_m(\varphi) g(\varphi)\right]^2. \quad [41]$$

By Fourier expansion of $P_0^{1/2}$ and G_m, the expression can be evaluated numerically. In Fig. 2, the correlation time of cos 2φ is plotted in units of D^{-1} against λ. Also shown are curves for the more commonly employed models of *free diffusion* and *site exchange.*

As it has been shown above, the exchange rate $1/\tau$ is given by $-1/3$ times the absolute value of the first nonvanishing eigenvalue γ_1 of the Smoluchowski operator. It can then be shown (*10*) that the cos 2φ correlation time is given by $1/3\tau$, or the inverse of $-\gamma_1$. This value is calculated numerically and plotted in Fig. 2.

The standard procedure in employing site-exchange models (*11*) is, however, not to evaluate $-\gamma_1$ exactly at all choices of λ, but rather to fit experimental spectra recorded at a range of temperatures to exchange rates, assuming these to be given by an Arrhenius type of relationship $Ae^{-V_3/kT}$ (*18–22*), where A is temperature independent. Above, the

exact values of $-\gamma_1$ for $\lambda > 10$ were fitted to an expression of this type, giving $A = 2.08D\lambda$. The error in extending this asymptotically obtained expression into the region of $\lambda < 10$ is observed in Fig. 2. The correlation time is greatly overestimated by the exchange model compared to that of the exact Smoluchowski model.

The correlation time calculated from the free-diffusion Wiener–Einstein model (*10*) is $1/(4D)$ which is also plotted in Fig. 2. Instead of approaching this value at small values of λ, the reciprocal of the first nonvanishing eigenvalue approaches $1/D$, the Wiener–Einstein operator eigenvalues in general being $-Dm^2$, $m = 0, \pm 1, \pm 2, \ldots$.

LIMITING CASES

In the limit of long correlation time, i.e., small D or low temperature, the two cases $\lambda \gg 1$ and $\lambda \ll 1$ are considered separately. In this limit, a ''powder''-type spectrum consisting of superimposed spectra from each individual stopped rotor in the sample is expected.

For simplicity, consider only the hyperfine interaction in the secular approximation, and set the hyperfine coupling constant a equal to 1. The energy levels are

$$E = 4m_s \sum_{n=-1}^{1} A_n(\varphi) m_{1_n}. \qquad [42]$$

where $A_n(\varphi) = 1/2 \cos^2(\varphi + n2\pi/3)$. Four of the eight EPR transitions are

$$\begin{aligned}
\nu_1 &= A_1(\varphi) + A_{-1}(\varphi) + A_0(\varphi),\\
\nu_2 &= A_1(\varphi) + A_{-1}(\varphi) - A_0(\varphi),\\
\nu_3 &= A_1(\varphi) - A_{-1}(\varphi) + A_0(\varphi),\\
\nu_4 &= -A_1(\varphi) + A_{-1}(\varphi) + A_0(\varphi). \qquad [43]
\end{aligned}$$

The remaining four are the negative values of these. When written in units of the hyperfine coupling constant a, the transitions are

$$\begin{aligned}
\nu_1 &= \frac{3}{2}, \quad \nu_2 = \frac{3}{2} - 2\cos^2\varphi,\\
\nu_3 &= \frac{1}{2} - \cos\left(2\varphi - \frac{2\pi}{3}\right),\\
\nu_4 &= \frac{1}{2} - \cos\left(2\varphi + \frac{2\pi}{3}\right). \qquad [44]
\end{aligned}$$

Consider a general stochastic variable x, with distribution $P(x)$. Consider also another stochastic variable f dependent on x through $f = f(x)$. The distribution $P(f)$ is then given by

$$P(f) = P(x)\frac{\partial x}{\partial f}. \qquad [45]$$

The transitions ν are dependent on the stochastic angle φ. The expected low-temperature spectrum is the distribution of transitions $P(\nu)$. This is the sum of the distribution of each individual transition.

First, consider the case where the potential is absent, $V_3 \ll kT$. Then, $P(\varphi) = 1/(2\pi)$. The distributions are calculated using the above formula and are observed to be

$$\begin{aligned}
P(\nu_1) &= \frac{1}{2\pi}\,\delta\left(|\nu_1| - \frac{3}{2}\right),\\
P(\nu_2) &= \frac{1}{2\pi}\,\frac{1}{\sqrt{(\frac{3}{4} - \frac{1}{2}\nu_2)(\frac{1}{4} + \frac{1}{2}\nu_2)}}, \quad \nu_2 \in \left\langle -\frac{1}{2}, \frac{3}{2}\right\rangle,\\
P(\nu_3) &= \frac{1}{2\pi}\,\frac{2}{\sqrt{1 - (\frac{1}{2} - \nu_3)^2}}, \quad \nu_3 \in \left\langle -\frac{1}{2}, \frac{3}{2}\right\rangle,\\
P(\nu_4) &= \frac{1}{2\pi}\,\frac{2}{\sqrt{1 - (\frac{1}{2} - \nu_4)^2}}, \quad \nu_4 \in \left\langle -\frac{1}{2}, \frac{3}{2}\right\rangle. \qquad [46]
\end{aligned}$$

The distributions of the other four transitions, which are the distributions $P(-\nu_1)$ to $P(-\nu_4)$ are also added. The unnormalized result is

$$\begin{aligned}
P(\nu) &= \frac{1}{\sqrt{1 - (\frac{1}{2} - \nu)^2}}, \quad \nu \in \left\langle +\frac{1}{2}, +\frac{3}{2}\right\rangle,\\
P(\nu) &= \frac{1}{\sqrt{1 - (\frac{1}{2} + \nu)^2}}, \quad \nu \in \left\langle -\frac{1}{2}, -\frac{3}{2}\right\rangle,\\
P(\nu) &= \frac{1}{\sqrt{1 - (\frac{1}{2} - \nu)^2}}\\
&\quad + \frac{1}{\sqrt{1 - (\frac{1}{2} + \nu)^2}}, \quad \nu \in \left\langle -\frac{1}{2}, +\frac{1}{2}\right\rangle. \qquad [47]
\end{aligned}$$

The spectrum calculated by using these formulas is shown in Fig. 3a. It should be compared to the low-temperature spectrum calculated using the SLE outlined above, which is shown in Fig. 3b.

It is observed that the 3b spectrum shows an approximate 3:1:1:3 ratio between the line amplitudes. However, the area under each transition line is equal. Thus, by adding extra

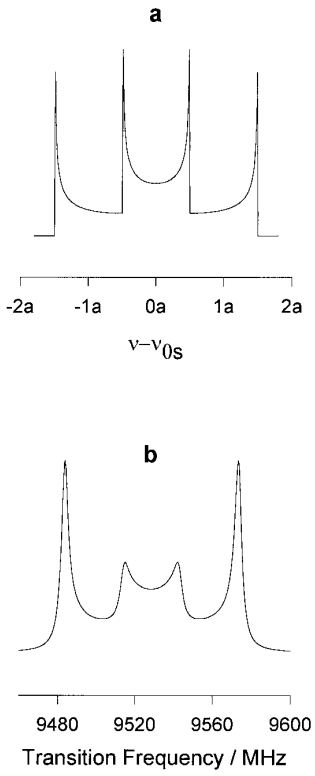

FIG. 3. Calculated rigid-limit EPR absorption-frequency spectrum of a single electron coupled to a free-diffusional methyl rotor. (a) Analytically calculated powder spectrum using the secular approximation. Transition frequency is in units of a, where the hyperfine interaction is $2a\cos^2\varphi$, and the electron Zeeman frequency is set to zero. (b) Spectrum calculated using the stochastic Liouville equation (SLE) with the Wiener–Einstein stochastic-process model. The electron Zeeman frequency is 9601.6 MHz, nuclear Zeeman frequencies are standard proton values, and the hyperfine coupling parameter a is 30 MHz. The diffusion constant, $D = kT/\xi$, is 0.01 MHz. The intrinsic broadening is set to 5 MHz.

intrinsic broadening to model other relaxation mechanisms, the line amplitudes can be brought to a 1:1:1:1 relationship. Heller (*3*) reports an experimental 1:1:1:1 spectrum in *x*-irradiated methyl malonic acid from the $CH_3\dot{C}(COOH)_2$ radical at 4.2 K. He claims an almost nonexistent potential barrier in this radical. The same intensity ratio is also predicted by the quantum mechanical free-rotor model at low temperatures (*3*). The correspondence is not trivial, since in the quantum-mechanical case, the Pauli principle for the nuclei must be taken into account to produce the correct spectrum. Such considerations are not made in the classical treatment in this work.

Second, the case is considered where a substantial potential barrier has stopped the rotor, $V_3 \gg kT$. In this case, the stopped rotors reside mainly in specific orientations, which are the potential wells $\varphi = 0, \pm 2\pi/3$. This situation is described by the assumed equilibrium distribution of angles $P(\varphi)$. Using [9, 46, 47], it is observed that (ν is in units of a):

$$P(\nu) = \frac{1}{\sqrt{1-(\frac{1}{2}-\nu)^2}}\, e^{-V_3/2kT}\cosh\left(\frac{V_3}{kT}\,\nu\sqrt{\frac{3}{4}-\frac{\nu}{2}}\right), \quad \nu \in \left\langle +\frac{1}{2}, +\frac{3}{2}\right\rangle,$$

$$P(\nu) = \frac{1}{\sqrt{1-(\frac{1}{2}+\nu)^2}}\, e^{-V_3/2kT}\cosh\left(\frac{V_3}{kT}\,\nu\sqrt{\frac{3}{4}+\frac{\nu}{2}}\right), \quad \nu \in \left\langle -\frac{1}{2}, -\frac{3}{2}\right\rangle,$$

$$P(\nu) = \frac{1}{\sqrt{1-(\frac{1}{2}-\nu)^2}}\, e^{-V_3/2kT}\cosh\left(\frac{V_3}{kT}\,\nu\sqrt{\frac{3}{4}-\frac{\nu}{2}}\right) + \frac{1}{\sqrt{1-(\frac{1}{2}+\nu)^2}}\, e^{-V_3/2kT}\cosh\left(\frac{V_3}{kT}\,\nu\sqrt{\frac{3}{4}+\frac{\nu}{2}}\right), \quad \nu \in \left\langle -\frac{1}{2}, +\frac{1}{2}\right\rangle. \qquad [48]$$

Because the result is nonnormalized, numerical constants have been removed for clarity. The spectrum obtained from using these formulas for a potential of $20kT$ is shown in Fig. 4a. It should be compared to the low-temperature spectrum obtained from the SLE lineshape calculation presented here, shown in Fig. 4b.

The processes studied in this work do not broaden the outer and inner lines of the commonly obtained 1:2:1:1:2:1 multiplet. However, by adding an intrinsic broadening representing relaxation due to other sources, the absorption spectrum shown in Fig. 4c is obtained from SLE.

In the limit of short correlation time, i.e., high temperature, motional equilibrium is effectively maintained during the progress of the experiment and the observed magnitudes of the hyperfine interactions are the averages of the $\{\cos^2(\varphi - 2\pi m/3), m = 0, \pm 1\}$ functions in the equilibrium distribution, all equal to $\frac{1}{2}$ regardless of potential depth. The expected spectrum of 1:3:3:1 ratio is obtained, as shown in Fig. 5. By spectrum calculations for reciprocals of correlation times up to $10\nu_{0S}$, shown in Figure 6, it is observed that the spectrum does not possess any motional broadening whatsoever

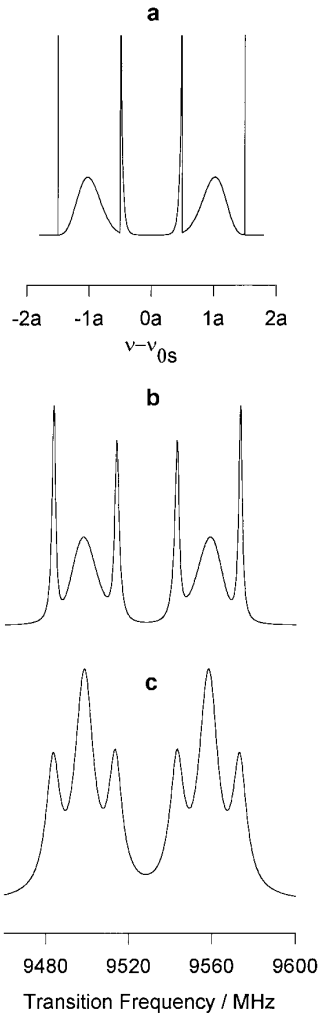

FIG. 4. Calculated rigid-limit EPR absorption spectrum of a single electron coupled to a diffusional rotor in a $20kT$ C_{3v} harmonic potential. (a) Analytically calculated powder spectrum using the secular approximation. Transition frequency is in units of a, where the hyperfine interaction is $2a\cos^2\varphi$, and the electron Zeeman frequency is set to zero. (b) Spectrum calculated using the Stochastic Liouville Equation with the Smoluchowski stochastic-process model. Electron Zeeman frequency is 9601.6 MHz, nuclear Zeeman frequencies are standard proton values, and the hyperfine coupling parameter a is 30 MHz. The diffusion constant, $D = kT/\xi$, is 0.005 MHz. The intrinsic broadening is set to 1 MHz. (c) As(b), but now with 5 MHz intrinsic broadening and with the potential increased to 100 kT to enhance resolution. The expected 1:2:1:1:2:1 sextet is observed.

when the reciprocal of the correlation time approaches and exceeds the electron Zeeman frequency ν_{0S}. Thus, ''lifetime broadening'' effects associated with other relaxation mechanisms are not observed with this model.

As is well known (*35–37*), the transition between the motionally averaged high temperature and the rigid-limit low-temperature spectrum occurs around the condition $\tau_c^{-1} \sim a$, at which the inner lines of the spectrum attain maximum broadening.

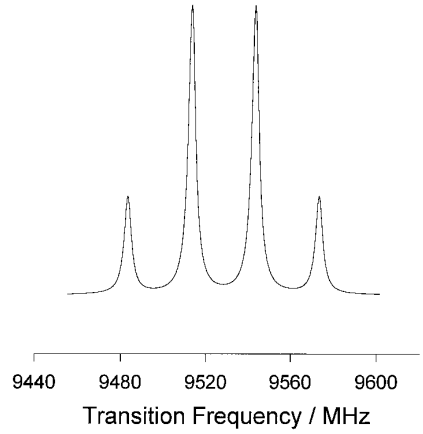

FIG. 5. Calculated extreme-narrowing-limit EPR absorption spectrum of a single electron coupled to a free-diffusional rotor. The spectrum is calculated using the stochastic Liouville equation with the Wiener–Einstein stochastic-process model. The electron Zeeman frequency is 9601.6 MHz, nuclear Zeeman frequencies are standard proton values and the hyperfine coupling parameter a is 30 MHz. The diffusion constant, $D = kT/\xi$, is 10,000 MHz. The intrinsic broadening is set to 5 MHz.

At a fixed potential of 10 kT ($\lambda = 10$), the correlation time is $\tau_c = 10^3/D$, observed from Fig. 2. The expected size of D for maximum broadening is therefore 4×10^4

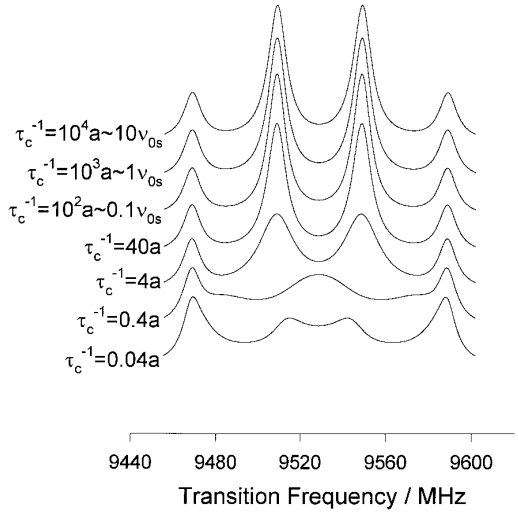

FIG. 6. Calculated EPR absorption spectra of a single electron coupled to a free-diffusional rotor. Spectra are calculated using the stochastic Liouville equation with the Wiener–Einstein stochastic-process model. The electron Zeeman frequency is 9601.6 MHz, nuclear Zeeman frequencies are standard proton values, and the hyperfine coupling parameter a is 40 MHz. A range of values are chosen for the diffusion constant, giving a spectrum of correlation times surrounding a^{-1} and the electron Zeeman frequency, ν_{0s}. It is observed that maximum broadening and breakdown of hyperfine structure occur at correlation time $\tau_c \sim a^{-1}$. It is further observed that no broadening change is observed near the condition $\nu_{0s}^{-1} \sim \tau_c$. Intrinsic broadening is set to 5 MHz, and for correlation times $\tau_c^{-1} \gg 0.1\nu_{0s}$, this is the only broadening observed.

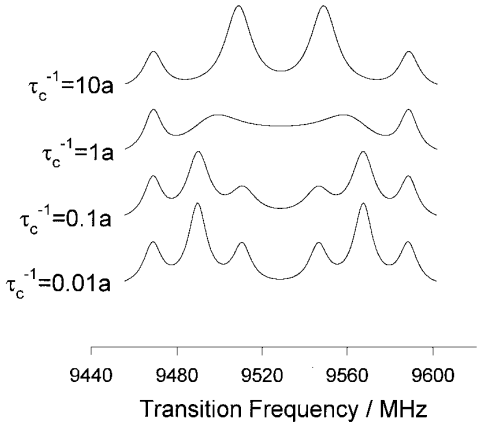

FIG. 7. Calculated EPR absorption spectra of a single electron coupled to a diffusional rotor in a $10kT$, C_{3v}, harmonic potential. Spectra are calculated using the stochastic Liouville equation with the Smoluchowski stochastic-process model. The electron Zeeman frequency is 9601.6 MHz, nuclear Zeeman frequencies are standard proton values, and the hyperfine coupling parameter a is 40 MHz. A range of values are chosen for the diffusion constant, giving a spectrum of correlation times surrounding a^{-1}. It is observed that maximum broadening and breakdown of hyperfine structure occur at correlation time $\tau_c \sim a^{-1}$. Intrinsic broadening is set to 5 MHz.

MHz. In Fig. 7, spectra recorded for choices of D surrounding this value are shown. Motional averaging is indeed observed to occur at this value.

In Fig. 6, the situation $V_3 = 0$ is considered, giving an expected correlation time of $1/(4D)$. The motion is then free diffusion. As for the previous case, the spectra still reveal maximum broadening around the condition $\tau_c^{-1} \sim a$. The inner pair of lines is merged to a single broad line under this condition.

DISCUSSION

Temperature Dependence of the Correlation Time

The present work suggests that there is a complicated relation between the correlation time and the temperature. In a wide experimental temperature range, it is possible that using only one of the limiting models is insufficient to describe the correct temperature dependence. In the relatively ''small,'' but practically significant, region $0.32 < V_3/kT < 5.62$, (Fig. 2), neither of the two approximate models, i.e., the *stepless diffusion* or the *jump model* may be applied. As an example, for a potential of 200 K, this corresponds to a temperature range of 35.6 up to 625 K.

In the jump-rate limit, the relation $A = 2.08DV_3/kT$ for the Arrhenius preexponential factor is obtained. If $D = kT/\xi$ is inserted, it is observed that there is no explicit temperature dependence left. The preexponential factor is, in general, dependent on the number of degrees of freedom of the motion, giving for example $A = D(V_3/kT)^{3/2}$ for a three-dimensional rotational-diffusion model (*39*), which results in an overall explicit temperature dependence. Note that the friction coefficient may contain an implicit temperature dependence, as for liquids, where the dependence is exponential (*40*).

Turning to the low potential limit, it is observed that the correlation time given by the free-diffusion model is $\tau_c = 1/(4D)$. According to the above discussion, there is a linear temperature dependence in D, as well as a possible exponential dependence. What is important is that neither the jump model nor the first eigenvalue of the Smoluchowski FP operator is correct here. The first greatly overestimates the correlation time, while the latter approaches a value four times larger than the free-diffusion value.

Bent Systems

In order to test the model on a realistic case, an experiment on irradiated acetic acid by Erickson *et al.* (*9*) is considered. The radical observed is CH_3COOD^-. For this system, previous investigations (*30, 38*) concluded that the radical geometry is nonplanar, so that the expression for the isotropic hyperfine interaction must be modified (*30*) by adding the term appearing in [15].

Erickson *et al.* report the three 77 K hyperfine couplings to be 0.0, 6.0, and 32.5 G. Assuming the methyl proton dihedral angles to be separated by 120° and assuming the form [13]–[15] of the hyperfine interactions, three equations are constructed, which are solved for the common hyperfine coupling parameters a, a_1, and the offset angle δ, giving $a = 12.8$ G, $a_1 = 8.06$ G, and $\delta = 108°$. Fitting the data to the regular Heller–McConnell-type expression [13] and [14], with only zero- and second-order terms, results in anomalous values of the parameters. In particular, a must be large and negative or a substantial and negative zero-order constant a_0 must be included.

Using the above calculated values in the lineshape simulation algorithm described in this work, the 77, 112, 132, and the 152 K spectra shown in Fig. 8 were obtained. They should be compared to experimental spectra along with the potential of $V_3 = 2.2$ kcal/mol given by Ericksson *et al.* (*9*) using a three site-exchange model, reported in the original paper. The experimental results were successfully simulated by the value of the potential found by Erickson *et al.*, showing that the site-exchange model is a good approximation. However, the present theory provides a more fundamental description of the structure and the dynamics by offering an interpretation of the empirical parameters used in the Arrhenius equation and in the diffusional limit.

CONCLUSIONS

It is observed that in the SLE formulation of the EPR lineshape from an unpaired electron spin coupled to a methyl

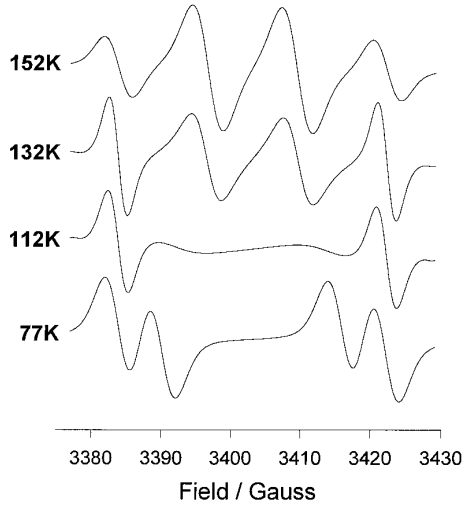

FIG. 8. Calculated EPR derivative magnetic field spectra of the radical CH_3COOD^- in irradiated acetic acid-d_1 at 77, 112, 132, and 152 K using the stochastic Liouville equation with the Smoluchowski-process model. The activation energy used is 2.2 kcal/mol after Erickson *et al.* (*9*), and the friction parameter is chosen as $\xi = 40$ to give optimal correspondence with experimental results (*9*). The electron Zeeman frequency was 9601.6 MHz, and the hyperfine coupling expression (*30*) $2a\cos^2(\varphi + \delta) + a_1\cos(\varphi + \delta)$, with a = 12.83 G, $a_1 = 8.057$ G, and $\delta = 108.3°$, was used.

rotor, the Smoluchowski process of Brownian motion in an external potential offers a unification of the previously employed processes, i.e., the site-exchange and the stepless-free-diffusion models.

The cos 2φ correlation time, on which motional averaging and linewidths are strongly dependent, is poorly represented by the extension of the free-diffusion model to low temperatures compared to the potential. Likewise, the extension of a site-exchange model into conditions of high temperature compared to the potential is inconsistent with the correlation time as calculated from the Smoluchowski model.

This work shows that quantitative calculations of the jump rate based on second-order expansion of the cosine potential are erroneous due to the overestimation of the actual barrier height. Numerically, the regular expression for the jump rate of the Arrhenius type [1] (*18–22*) is found, with a preexponential factor of approximately 2.08 DV_3/kT.

It is seen that the maximum broadening of inner lines when $\tau_c^{-1} \sim a$ in the free-diffusion case is accompanied by the breakdown of the inner doublet. We have not found experimental reports in the literature supporting this observation.

Even though the nonsecular terms of the Hamiltonian are included, no lifetime broadening effects (*41*) are observed for the high-field simulations of this work, in agreement with the regular behavior of exchange of isotropic systems within the simpler lineshape models of site exchange and within the Redfield relaxation theory.

APPENDIX A: SYMMETRY CONSIDERATIONS

The symmetry group of the stochastic operator is C_{3v}. This includes the C_3 rotations 0 and $\pm 2\pi/3$, as well as the parity operator $Pf(\varphi) = f(-\varphi) = g(\varphi)$, which also is the reflection operator about the line $\varphi = 0$. The reflections about $\varphi = \pm 2\pi/3$ are the combinations of the remaining two C_3 rotations with the reflection operator.

There are three representations, A_1, A_2, and E, of which the last is two-dimensional. As a representation of the subgroup C_3, both A_1 and A_2 are identified with the symmetric representation of C_3, A_1. The E representation of C_{3v} can be reduced to the $E_a \oplus E_b$ representation of C_3.

Using projection operators, the components of a general complex Fourier basis function transforming as the basis of the irreducible representations are found. The basis for the A_1 representation is $1/\sqrt{2\pi} \cup \{(1/\sqrt{\pi})\cos 3m\varphi \,|\, m \in N\}$, for the A_2 it is $\{(1/\sqrt{\pi})\sin 3m\varphi \,|\, m \in N\}$, while it for E is $\{(1/\sqrt{\pi})\cos[(3m \pm 1)\varphi] \,|\, m \in N\} \cup \{(1/\sqrt{\pi})\sin[(3m \pm 1)\varphi] \,|\, m \in N\}$.

A high degree of approximate degeneracy will occur between A_1 and A_2 levels as the representation matrices differ only by six elements; denoting by index 0, the constant $1/\sqrt{2\pi}$ and indexing other basisfunctions by the integer m, they are the (0, 0), (0, 1), (0, 2), (1, 0), (2, 0), and (1, 1) elements.

APPENDIX B: BASIS TRANSFORMATIONS

The real Fourier basis, which is employed, is not as convenient for practical calculations as the complex Fourier basis. The real Fourier basis can be related to the complex basis by the general formula

$$\psi_m = \frac{1}{2\sqrt{\pi\alpha_m}}(e^{im\varphi} + \alpha_m e^{-im\varphi}),$$
$$\alpha_m = e^{i[(3/2)\zeta_m + (1/2)]\pi},$$
$$\zeta_m = \begin{cases} 1, & m > 0 \\ -1, & m < 0. \\ 0, & m = 0 \end{cases} \qquad [49]$$

The cosine basis function are labeled here by $m > 0$, while the sine basis functions are labeled by $m < 0$.

The SL operator can be transformed to this basis from the complex basis by virtue of

$$L_{RF} = \mathbf{R} L_{CB} \mathbf{R}^+. \qquad [50]$$

Here, L_{RF} and L_{CB} refer to the real and complex bases, respectively, and $\mathbf{R}$ is given by

$$\mathbf{R} = \frac{1}{\sqrt{2}} \begin{bmatrix} \ddots & & & & & & \iddots \\ & 1 & & & & 1 & \\ & & 1 & & 1 & & \\ & & & \sqrt{2} & & & \\ & & i & & -i & & \\ & i & & & & -i & \\ \iddots & & & & & & \ddots \end{bmatrix}. \quad [51]$$

APPENDIX C: GENERAL EXPRESSION FOR THE FOURIER COEFFICIENTS OF $P_0^{1/2}$

The program can easily be organized so that the potential offset angle δ in [17] can be included in the hyperfine term only. Then the expression [22] for the equilibrium distribution coefficients is sufficient. The general expression where a nonzero angle is used in the square root of the equilibrium distribution is, however, useful when calculating [36], and is therefore reported:

$$c_{3m} = 2\sqrt{\pi}\cos(3m\delta)e^{-V_3/4kT}I_m\left(\frac{V_3}{4kT}\right),$$

$$c_0 = \sqrt{2\pi}e^{-V_3/4kT}I_0\left(\frac{V_3}{4kT}\right),$$

$$c_{3-m} = 2\sqrt{\pi}\sin(3m\delta)e^{-V_3/4kT}I_m\left(\frac{V_3}{4kT}\right). \quad [52]$$

ACKNOWLEDGMENTS

This work was financed by the Norwegian Research Council (NFR) and the Swedish Natural Science Council (NFR). The project has benefited greatly from a travel grant by the Nordic Academy of Research Education (NorFA) and was supported by the Norwegian National Supercomputing Resource. We are grateful to Professor Anders Lund and Professor Einar Sagstuen for their continuing interest, eager advice, and generous supply of relevant literature. N. P. Benetis also thanks D. J. Schneider for letting him in on the secrets of the Lanczos algorithm.

REFERENCES

1. A. Horsfield, J. R. Morton, and D. H. Whiffen, *Mol. Phys.* **4,** 425 (1961).
2. A. Horsfield, J. R. Morton, and D. H. Whiffen, *Mol. Phys.* **5,** 115 (1962).
3. C. Heller, *J. Chem. Phys.* **36,** 175 (1962).
4. I. Miyagawa and K. Itoh, *J. Chem. Phys.* **36,** 2157 (1962).
5. R. B. Davidson and I. Miyagawa, *J. Chem. Phys.* **52,** 1727 (1970).
6. D. M. Close, R. V. Lloyd, and W. A. Bernhard, *J. Chem. Phys.* **72,** 2203 (1980).
7. M. Brustolon, T. Cassol, L. Micheletti, and U. Segre, *Mol. Phys.* **61,** 249 (1987).
8. S. Clough and F. Poldy, *J. Chem. Phys.* **51,** 2076 (1969).
9. R. Erickson, U. Nordh, N. P. Benetis, and A. Lund, *Chem. Phys.* **168,** 91 (1992).
10. J. H. Freed and G. K. Fraenkel, *J. Chem. Phys.* **39,** 326 (1964).
11. J. H. Freed, *J. Chem. Phys.* **43,** 1710 (1965).
12. L. D. Favro, *in* ''Fluctuation Phenomena in Solids'' (R. E. Burgess, Ed.), Academic Press, New York, 1965.
13. P. L. Nordio and P. Busolin, *J. Chem. Phys.* **55,** 5485 (1971).
14. P. L. Nordio, G. Rigatti, and U. Segre, 1972, *J. Chem. Phys.* **56,** 2117 (1972).
15. C. F. Polnaszek, G. V. Bruno, and J. H. Freed, *J. Chem. Phys.* **58,** 3185 (1973).
16. J. H. Freed, *in* ''Spin Labelling: Theory and Applications'' (L. J. Berliner, Ed.) Academic Press, New York, 1976.
17. M. v. Smoluchowski, *Ann. Phys.* **31,** 1103 (1915).
18. H. A. Kramers, *Physica* **7,** 284 (1940).
19. R. Landauer and J. A. Swanson, *Phys. Rev.* **121,** 1668 (1961).
20. C. Blomberg, *Physica* **86A,** 49 (1977).
21. D. L. Weaver, *Phys. Rev.* **20B,** 2558 (1979).
22. S. Dattagupta, ''Relaxation Phenomena in Condensed Matter Physics,'' Chap. 13, Academic Press, New York, 1987.
23. R. Kubo, *in* ''Advances in Chemical Physics'' (K. E. Schuler, Ed.), Vol. 16, p. 101, Krieger, Huntington, New York, 1969.
24. J. H. Freed, G. V. Bruno, and C. F. Polnaszek, *J. Phys. Chem.* **75,** 3385 (1971).
25. J. H. Freed, *in* ''Electron Spin Relaxation in Liquids'' (L. T. Muus and P. W. Atkins, Eds.), Plenum, New York, 1972.
26. C. Lanczos, *J. Res. Natl. Bur. Stand.* **45,** 255 (1950); **49,** 33 (1952).
27. N. P. Benetis, A. Schneider, and J. H. Freed, *J. Magn. Reson.* **85,** 275 (1988).
28. S. Dattagupta, ''Relaxation Phenomena in Condensed Matter Physics,'' Chap. 12, Academic Press, New York, 1987.
29. R. Kubo, M. Toda, and N. Hashitsume, ''Statistical Physics II,'' Section 2.5, Springer-Verlag, Berlin, 1978.
30. D. Suryanarayana and M. D. Sevilla, *J. Phys. Chem.* **84,** 3045 (1980).
31. J. G. Powles and H. S. Gutowsky, *J. Chem. Phys.* **23,** 1692 (1954).
32. E. Butkov, ''Mathematical Physics,'' Addison–Wesley, Reading, Massachusetts, 1968.
33. J. Villain, *Le J. de Phys.* **36,** 581 (1975).
34. N. Fjeldsø, ''The Supersymmetric Quantum Pendulum,'' Thesis, Department of Physics, University of Oslo, 1989.
35. N. M. Atherton, ''Principles of Electron Spin Resonance,'' Section 9.7, Ellis Horwood PTR Prentice Hall, New York, 1993.
36. R. Lenk, ''Brownian Motion and Spin Relaxation,'' Section 5.1.3, Elsevier, Amsterdam, 1977.
37. A. Abragam, ''The Principles of Nuclear Magnetism,'' Chap. 10, Section IV, Clarendon Press, Oxford, 1961.
38. J. E. Bennet and L. H. Gale, *Trans. Faraday Soc.* **64,** 1174 (1968).
39. S. Dattagupta, ''Relaxation Phenomena in Condensed Matter Physics,'' Chap. 7, Academic, New York, 1987.
40. P. S. Hubbard, *Phys. Rev.* **131**(3), 1155 (1963).
41. D. Kivelson, *in* ''Electron Spin Relaxation in Liquids'' (L. T. Muus and P. W. Atkins, Eds.), Chap. 10, Plenum, New York, 1972.